PERMAFROST AND PERIGLACIAL PROCESSES
Permafrost and Periglac. Process. **20**: 235–256 (2009)
Published online 4 August 2009 in Wiley InterScience
(www.interscience.wiley.com) DOI: 10.1002/ppp.656

Physical and Ecological Changes Associated with Warming Permafrost and Thermokarst in Interior Alaska

T. E. Osterkamp,[1]* *M. T. Jorgenson*,[2] *E. A. G. Schuur*,[3] *Y. L. Shur*,[4] *M. Z. Kanevskiy*,[5] *J. G. Vogel*[3] *and V. E. Tumskoy*[6]

[1] Geophysical Institute, University of Alaska, Fairbanks, AK, USA
[2] ABR, Inc., Fairbanks, AK, USA
[3] Department of Botany, University of Florida, Gainesville, FL, USA
[4] Department of Civil and Environmental Engineering, University of Alaska, Fairbanks, AK, USA
[5] Institute of Northern Engineering, University of Alaska, Fairbanks, AK, USA
[6] Department of Geology, Moscow State University, Moscow, Russia

ABSTRACT

Observations and measurements were made of physical and ecological changes that have occurred since 1985 at a tundra site near Healy, Alaska. Air temperatures decreased (1985 through 1999) while permafrost warmed and thawed creating thermokarst terrain, probably as a result of increased snow depths. Permafrost, active layer and ground-ice conditions at the Healy site are the result of the interaction of climatic, ecologic and other factors. The slow accumulation of ground ice in an intermediate permafrost layer formed by upward freezing from the permafrost surface leads to long-term differential frost heave and microrelief. When ground ice in the permafrost melts, the ground surface settles differentially resulting in thermokarst terrain (pits, gullies). Windblown snow fills the thermokarst depressions causing further warming and thawing of the underlying permafrost — a positive feedback effect that enhances permafrost degradation. Thermokarst-induced changes in relief alter the near-surface hydrology and ecological processes. Changes in vegetation included differential tussock growth and mortality and a shift in moss species abundance and relative productivity, depending on microtopographic position created by the thermokarst terrain. Water redistribution towards thermokarst depressions caused adjacent higher areas to become drier and resulted in increased moss mortality and shrub abundance. Copyright © 2009 John Wiley & Sons, Ltd.

KEY WORDS: permafrost; thermokarst; climate change; ecology; vegetation

INTRODUCTION

Permafrost regions occupy 20–25 per cent of the exposed land surface of the northern hemisphere (Zhang *et al.*, 1999) and 80 per cent of Alaska (Jorgenson *et al.*, 2008). Much of this permafrost is warm, within a few degrees of thawing. Climate in Alaska warmed beginning in the late 1800s coincident with an increase in global air temperatures (Hansen and Lebedev, 1987). During the 20th century, air temperatures increased until about 1940, decreased during the third quarter and increased sharply at the beginning of the fourth quarter (Bowling, 1990). Temperatures from the late 1970s to the end of the 20th century mostly warmed, but some stations show little or no warming or even a cooling

* Correspondence to: T. E. Osterkamp, Geophysical Institute, University of Alaska, Fairbanks, AK, 99775-7320.
E-mail: ffteo@uaf.edu

Received 20 November 2008
Revised 1 May 2009
Accepted 6 May 2009

(Osterkamp, 2007a, 2007b, 2008). The first few years of the 21st century have been warmer.

Permafrost in northern Alaska responded to the century-long warming of air temperatures and changes in snow cover by warming about 2 to 4°C at its surface beginning in the early 1900s, although a few sites showed little or no change or cooled (Lachenbruch and Marshall, 1986; Lachenbruch *et al.*, 1988; Zhang and Osterkamp, 1993; Osterkamp and Jorgenson, 2006). Sparse data on thermokarst indicate that this warming also occurred in Interior Alaska (Osterkamp, 2005).

During the last quarter of the 20th century, permafrost appears to have warmed statewide with some exceptions (Clow and Urban, 2002; Osterkamp, 1994, 2003a, 2005, 2007a, 2008; Osterkamp and Romanovsky, 1999). At the surface of the permafrost, the magnitude of this warming was 3 to 4°C for the Arctic Coastal Plain, 1 to 2°C for the Brooks Range including its northern and southern foothills and 0.3 to 1°C south of the Yukon River. The warming was seasonal (primarily in winter) with little change in summer conditions and active-layer thicknesses. Snow cover effects account for about one half of this permafrost warming at Barrow (Stiegliz *et al.*, 2003) and have been partially to almost totally responsible for permafrost warming at other sites (Osterkamp, 2007a, 2007b).

Climatic change since the mid-1800s has resulted in widespread thermokarst terrain in the relatively 'warm' zone of discontinuous permafrost (Osterkamp *et al.*, 2000; Jorgenson *et al.*, 2001). In the Arctic, in the colder zone of continuous permafrost where permafrost has been regarded as stable, new evidence indicates there has been a recent and abrupt increase in the degradation of ice wedges (Jorgenson *et al.*, 2006). If the climate warms another 5–8°C over the next century, then most of the permafrost in Alaska will be degrading.

Permafrost thawing can be initiated by climatic change (e.g. warming air temperatures, snow cover effects, changing precipitation) (Froese *et al.*, 2008) and surface disturbances (e.g. wildfire, flooding, human activities). Thawing of ice-rich permafrost results in thermokarst terrain that causes substantial ecosystem and human impacts (Washburn, 1978). Thermokarst in forests in lowland areas can lead to the partial or wholesale conversion of ecosystems from terrestrial to aquatic or wetland ecosystems, and in upland areas can influence slope stability resulting in landslides and erosion (Osterkamp *et al.*, 2000; Vitt *et al.*, 2000; Jorgenson *et al.*, 2001; Huscroft *et al.*, 2004; Shur and Osterkamp, 2007). Human impacts include changes in the habits and type of animals used as food sources and loss of infrastructure integrity (Brown and Grave, 1979; Huntington, 1992; Osterkamp *et al.*, 1997).

Permafrost formation and degradation are processes in which climate plays an important role; however, ecosystem processes also play a significant role (Shur and Jorgenson, 2007). The upper permafrost evolves along with vegetative succession, accumulation of soil organic matter, thinning of the active layer and accumulation of ground ice (Shur, 1988). Upon thawing, the patterns, extent, and rates of physical and ecological changes associated with thermokarst are closely related to the dynamics of ground-ice evolution. Modes of permafrost degradation and the ecological consequences depend on the interaction of slope position, soil texture, hydrology and ice content (Jorgenson and Osterkamp, 2005).

A permafrost observatory was established near Healy in 1985 for the purpose of investigating the response of permafrost to climate (Osterkamp, 2003b). Initially, it consisted of an access hole for deep temperature measurements. Provisions were made later for air, ground surface and permafrost surface temperature measurements. Detailed ecological studies were initiated in 2003 (Schuur *et al.*, 2007) and soil and ground-ice studies in 2005. A unique feature of this site is that there was no thermokarst terrain in the immediate area of the borehole in 1985; however, new thermokarst terrain developed there and in adjacent areas during the period of observations. This has resulted in a rare opportunity to investigate the complex interactions between ecological processes and permafrost and thermokarst dynamics at a site where thermokarst terrain has developed and continues to do so.

This paper summarises and integrates measurements and observations of the physical and ecological changes that have occurred at the Healy site as a result of variations in climate that caused warming and thawing of permafrost and the development of thermokarst terrain. Field and remote-sensing measurements of these changes allowed us to assess the interactions of air temperatures and snow on permafrost thermal regimes, the consequences of increasing permafrost temperatures and ground-ice distribution on active-layer dynamics and thermokarst, and the impacts of thermokarst terrain on water redistribution, peat accumulation and shifting vegetation composition. The results provide insights into the processes, dynamics, direction and magnitude of the changes. However, the study is incomplete because the processes and associated changes are still occurring, will continue for a very long time and will undoubtedly reveal new unexpected consequences of permafrost degradation.

DOI: 10.1002/ppp

SITE CHARACTERISTICS AND METHODS

Site Description

The observatory is located at 63° 52′ 42.1″ N, 149° 15′ 12.9″ W (elevation 690 m) in the foothills north of the Alaska Range north of Denali National Park and about 15 km west of Healy. It is north and east of the Stampede Trail and south of Eight Mile Lake (Figure 1) in an area of tundra that slopes gently to the north and east. The hilltops have gravelly soils associated with glacial till and are covered by a thin aeolian silt cap. The lower slopes and valleys have thick peat accumulations over fine-grained soils associated with colluvial deposits. Water tracks are visible in a recent aerial photo (Figure 1). The borehole site was placed at what later became the intersection of two water tracks. Thaw settlement in these water tracks and the resulting downstream thermokarst gully indicate that the underlying soil is more ice-rich than the adjacent tundra.

The vegetation in this area is dominated by moist acidic tussock tundra comprised of sedge (*Eriophorum vaginatum*), deciduous and evergreen shrubs

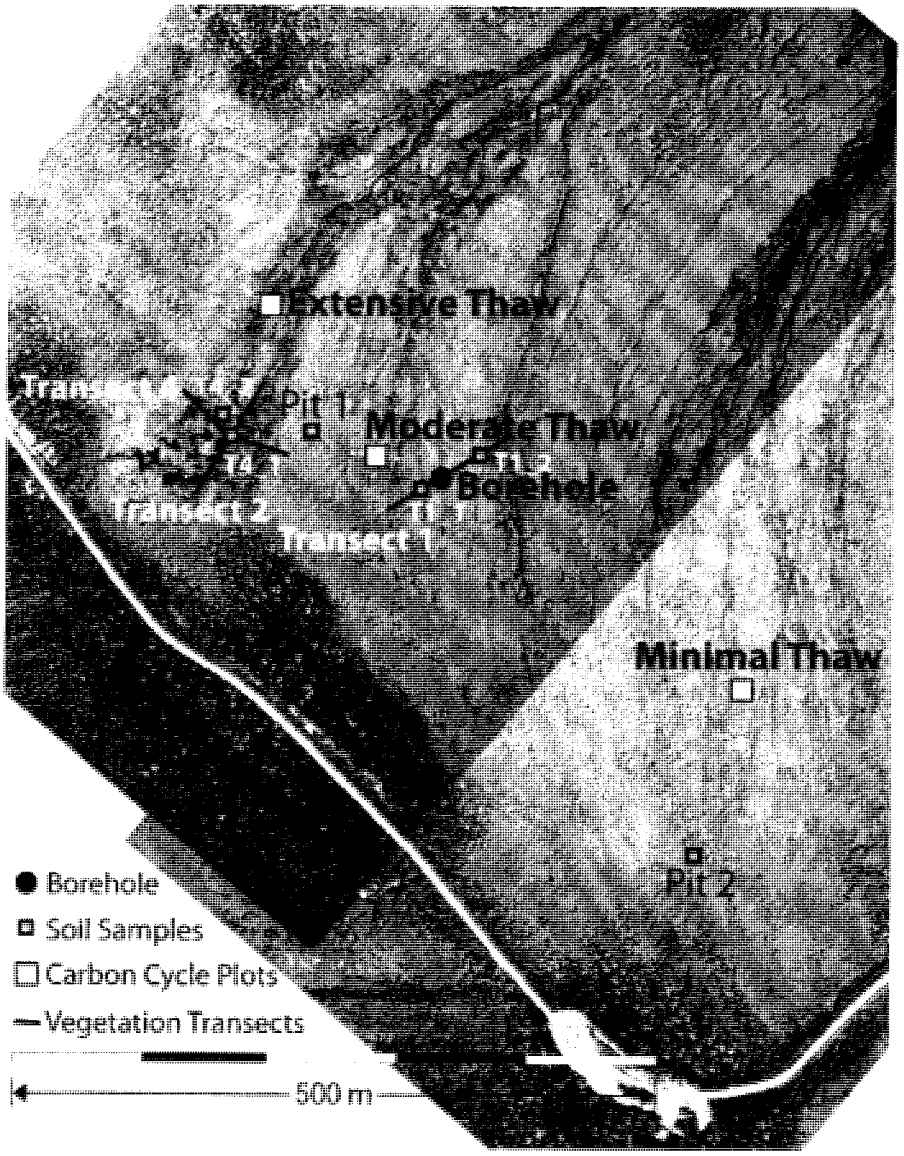

Figure 1 Aerial photograph of the Healy site (north of Denali National Park and about 15 km west of the village of Healy) taken in 2003 showing the locations of the various thaw sites, borehole, pits and transects. The top of the figure is north.

DOI: 10.1002/ppp

(*Vaccinium uliginosum, Rubus chamaemorus, Betula nana* and *Ledum palustre*), and abundant mosses (*Sphagnum* spp. and feathermoss). Areas that have subsided due to thermokarst development tend to have increased shrub biomass and productivity at the expense of the graminoids (Schuur *et al.*, 2007). This area is at or near treeline, so *Picea glauca* occurs more commonly in the riparian areas and rarely scattered within the tundra.

The nearest meteorological station is at Healy (elevation 454 m). Snow covers the ground from mid-September through mid-May. For the period from 1980 to 2003, the mean air temperature was −1.3°C, and mean of the maximum annual snow depths was 0.52 m (Figure 2).

A 30-m borehole for measuring permafrost temperatures was drilled in 1985 using a rotary air drill. The soil profile consisted of about 1/2 m of peat at the surface, 5 m of ice-rich silt and 23 m of gravel with boulders underlain by sand. A galvanised iron pipe (2 cm in diameter) capped at the bottom was placed in the hole to provide access for temperature logging (Osterkamp, 2003b). Two holes (1-m depth) for measuring permafrost surface temperatures were hand drilled in 1995; one about 1 m from the borehole and the other on the adjacent tundra about 5 m distant.

Temperature Measurements

Borehole temperatures were measured annually, except for 1986–88 and 1992, using a single thermistor sensor on a cable with a maximum sensitivity of 0.003°C and a typical accuracy of about 0.01°C (Osterkamp, 2003b). Air temperatures (in a radiation shield at 1.5-m height), and ground surface (2 to 5-cm depth) and permafrost surface temperatures (0.1–0.3 m below the permafrost surface) were monitored with miniature data loggers (Osterkamp, 2003b; Osterkamp and Jorgenson, 2009) with an accuracy of about 0.2°C. To assess differences in ground surface temperatures associated with stable and degrading permafrost, pairs of sensors were placed just under the surface of the vegetation at the Extensive Thaw site (old thermokarst terrain): one in a thermokarst depression and one a few metres distant on the stable tundra.

Soil and Ground Ice

Soil and ground-ice studies were used to obtain information on permafrost and active-layer dynamics. Three transects, 150 m in length, were set up across a toposequence of ecosystems associated with

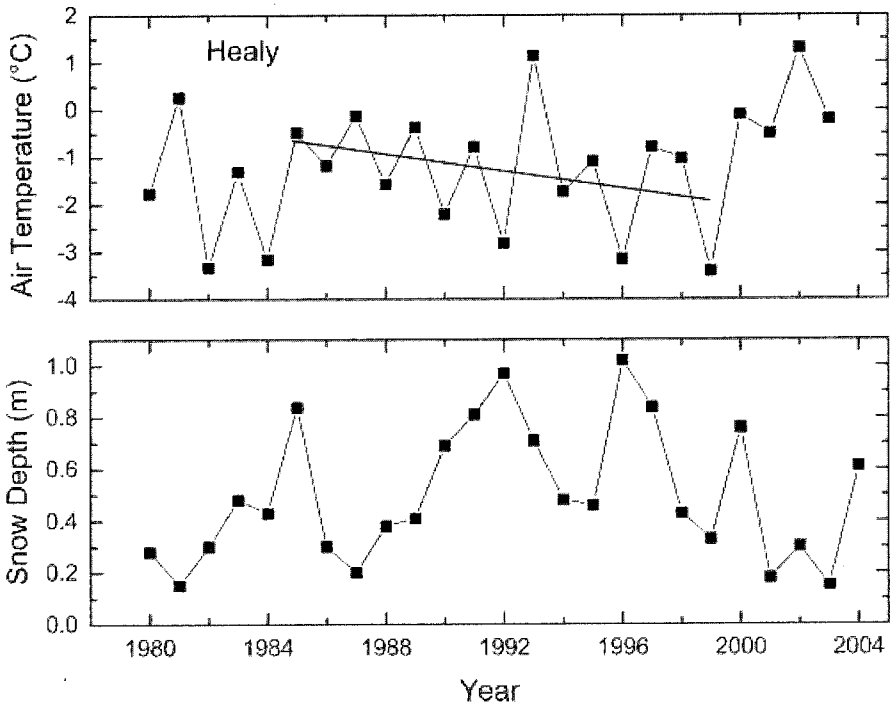

Figure 2 Annual mean air temperatures and maximum snow depths from 1980 to 2004 for Healy, Alaska. The straight line in the air temperature data (1985–99) is a linear fit to the data for the period from 1985 through 1999. Permafrost temperatures warmed from 1985 through 1998.

DOI: 10.1002/ppp

permafrost degradation (Figure 1). Ground and water elevations, vegetation, soils, ground ice and permafrost were studied at up to three sites along each transect. Vegetation at each plot was described by making visual estimates of the per cent cover of the dominant species. Soil cores and pits were used to determine surface organic thickness, the texture of each horizon, mineral characteristics, depth of organic matter, depth of thaw, and visible ice volume and structure. For determining ice volume, frozen samples were taken every 0.2 m along the cores and photographed. Samples were analysed for volumetric and gravimetric water content, electrical conductivity and pH. The soil was described using standard NRCS procedures, and ground ice was described and classified using a system appropriate for Alaskan soils (Shur and Jorgenson, 1998).

Thermokarst

The occurrence, distribution and characteristics of thermokarst terrain were investigated with measurements of ground surface elevations, ground-ice volumes, soil densities and time series of aerial photography. The access pipe for temperature measurements on Transect 1 served as a fixed datum (about 690 m) with measurements made in 1996, 1997, 2003 and 2005 referenced to the pipe datum. Thaw settlement in pits along transects was estimated by comparing elevations of the pits with the elevations of surrounding terrain. Measured ground-ice volumes and soil densities were used to calculate the potential thaw settlement:

$$S = \frac{(H_2 - H_1)\delta}{1 - \delta} \tag{1}$$

where H_1 and H_2 are the active-layer depths before and after thermokarst and:

$$\delta = ((\gamma_{dt} - \gamma_{df})/\gamma_{dt}) \tag{2}$$

where γ_{df} is the dry density of the frozen soil sample, and γ_{dt} is the dry density of the thawed and consolidated sample under overburden soil pressure (Crory, 1973). Equation 1 was derived for homogeneous soil or for soil that can be represented by an average thaw strain. For the layered sequence of upper permafrost with highly variable thaw strain, thaw settlement was calculated using:

$$\Delta S_i = h_i\delta_i \text{ and } \Delta H_i = h_i - h_i\delta_i \tag{3}$$

where h_i is a sub-layer with uniform thaw strain, δ_i, and ΔH_i is the thickness of the sub-layer h_i after thawing and settling. Thaw settlement stops when the combined thickness of sub-layers affected by thawing and settling reaches the difference between old and new equilibrium depths of the active layer or:

$$\sum_{i=1}^{n} (h_i - h_i\delta_i) = H_2 - H_1 \tag{4}$$

Equations 3 and 4 were used to calculate potential thaw settlement for each core across a range of equilibrium thaw depths to the bottom of the core.

Thermokarst features were mapped for 1954, 1981 and 2005 based on photo-interpretation of associated microtopographic and vegetative patterns. The 1954 and 1981 airphotos were scanned by the USGS Eros Data Center, and the 2005 airphotos were obtained using a fixed-wing aircraft. Once georectified, thermokarst features were delineated by onscreen digitising using ESRI ArcMap software and classified according to the system of Jorgenson and Osterkamp (2005). Further details regarding methods for the soil, ground ice and thermokarst studies are given in Osterkamp and Jorgenson (2009).

Vegetation

Another vegetation survey was conducted to determine the ground area occupied by different vascular and non-vascular plant species at each of three sites (Minimal Thaw, Moderate Thaw and Extensive Thaw, Figure 1) that differed in quantity and age of thermokarst terrain. Twelve large quadrats per site distributed in pairs across a 40-m transect were sampled using a 0.7×0.7 m frame. A line-intercept method was used to quantify the abundance of five dominant moss groups and the vascular plant species *E. vaginatum*. Other vascular plant species were not quantified here because they grow up out of the moss understory and do not occupy ground area to the exclusion of other species. A description of vegetation biomass and productivity can be found in Schuur *et al.* (2007).

Dead moss samples were collected during the summers of 2003 and 2005 and analysed for radiocarbon to determine the age at death. While both sets of data are useful for overall site interpretation, the 2003 sampling effort likely oversampled the Minimal Thaw site with the least dead moss, whereas the 2005 sampling effort was randomly distributed and more representative of each site.

Living *Sphagnum* spp. samples were collected as isotope reference samples at each site. Live and dead moss samples were processed for cellulose extraction.

Individual moss bodies from a sample were divided into 0.5-cm segments starting at the moss surface (defined as the top of the capitulum). Segments were isolated from individual moss bodies and corresponding segments were combined within a sample that typically consisted of 20 to 50 individual moss bodies. Each of the segments for all moss samples was subjected to sequential extraction procedures that removed C compounds, producing holocellulose (Gaudinski *et al.*, 2005). Cellulose extraction was done to isolate the structural C from more recent photosynthate in order to determine the final year of growth. The ^{14}C results are expressed as $\Delta^{14}C$ after correcting for any fractionation of ^{13}C (Stuiver and Polach, 1977) yielding $\Delta^{14}C$ measurements that vary only as a function of age. Radiocarbon measurements of dead moss were used in combination with the change in the atmospheric radiocarbon content over the last 40 years to infer the age at death for these mosses (Levin and Kromer, 1997).

RESULTS AND DISCUSSION

An interacting sequence of permafrost and ecological changes in response to changing air temperatures and snow cover was found. The timing and amount of permafrost degradation was closely associated with changing permafrost temperatures and snow covers, ground-ice characteristics and active-layer dynamics. Permafrost degradation altered surface topography, surface and ground water levels, and channelisation of surface runoff. The differential thaw settlement and redistribution of water caused shifts in vegetation and peat accumulation in response to wetting and drying. The timing of these vegetation changes was assessed using radiocarbon dating of dead mosses. These interactions are described in more detail below.

Air Temperatures and Snow Cover

A comparison of air temperatures measured periodically at the site with those at Healy show that the site was typically colder than Healy from March through October and warmer from November through February (Figure 3). Annual mean air temperatures at the site averaged −2.4°C (1996–98), about 0.7°C less than Healy. A linear fit to the data (Figure 2) for the period from 1985 through 1999 shows a decrease of 1.5°C or about 0.1°C per year, although 1993 was an unusually warm year. In contrast, the 4 years from 2000 to 2003 were very warm because of warm winters.

Snow depths were not measured at the site, although occasional estimates made during the 1990s indicate a range of about 0.1 to 0.5 m with larger depths predominant. Measured snow depths at Healy (Figure 2) and throughout Interior Alaska were much

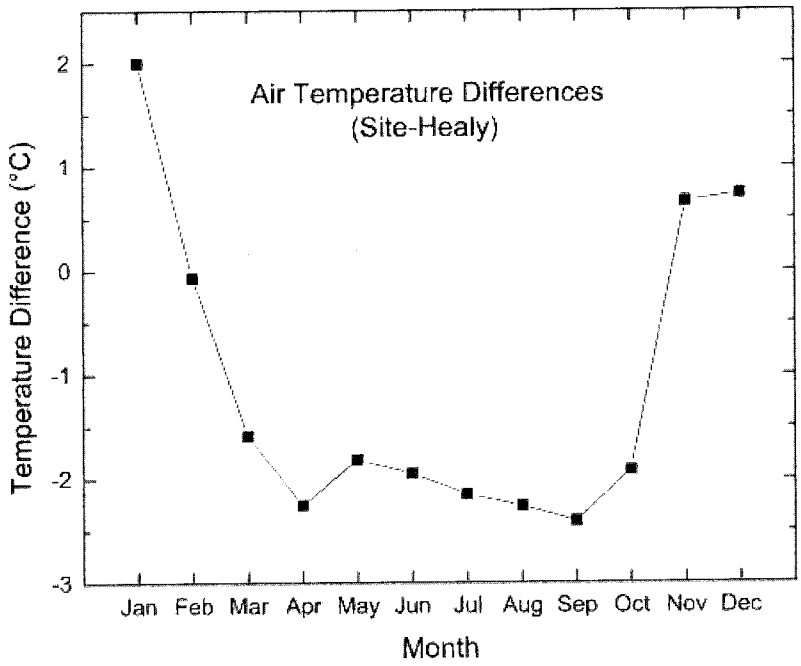

Figure 3 Differences in monthly mean air temperatures between the site and the village of Healy, Alaska.

DOI: 10.1002/ppp

greater during the 1990s compared to the 1980s (Osterkamp, 2007a).

Ground Surface Temperatures

Figure 4 and Table 1 show data from a paired site (thermokarst depression and nearby tundra). Ground surface temperatures on the tundra in the Extensive Thaw site remained significantly below freezing, typically from early October to late April. There were multiple freezing and thawing events for several weeks prior to and after this period. Annual mean ground surface temperatures in the old thermokarst depressions ranged from 2–4°C warmer than on the nearby tundra. This was a result of mean winter temperatures that were close to 0°C, 3–6°C warmer in the depressions compared to the tundra. These large differences were attributed to surface characteristics and snow. Thermokarst depressions were generally filled with vegetation (sedges and moss), with sedges extending 0.1 m or more above the wet moss or water surface (up to 0.4 m below the surrounding tundra surface). Winter observations showed that snow was redistributed by wind, filling the depressions. The increased snow thickness in depressions provides additional insulation for the ground surface causing it to be warmer than the surrounding tundra (Stieglitz *et al.*, 2003; Kershaw, 2008), retarding and reducing ground freezing and enhancing permafrost warming and thawing and talik development (i.e. the formation

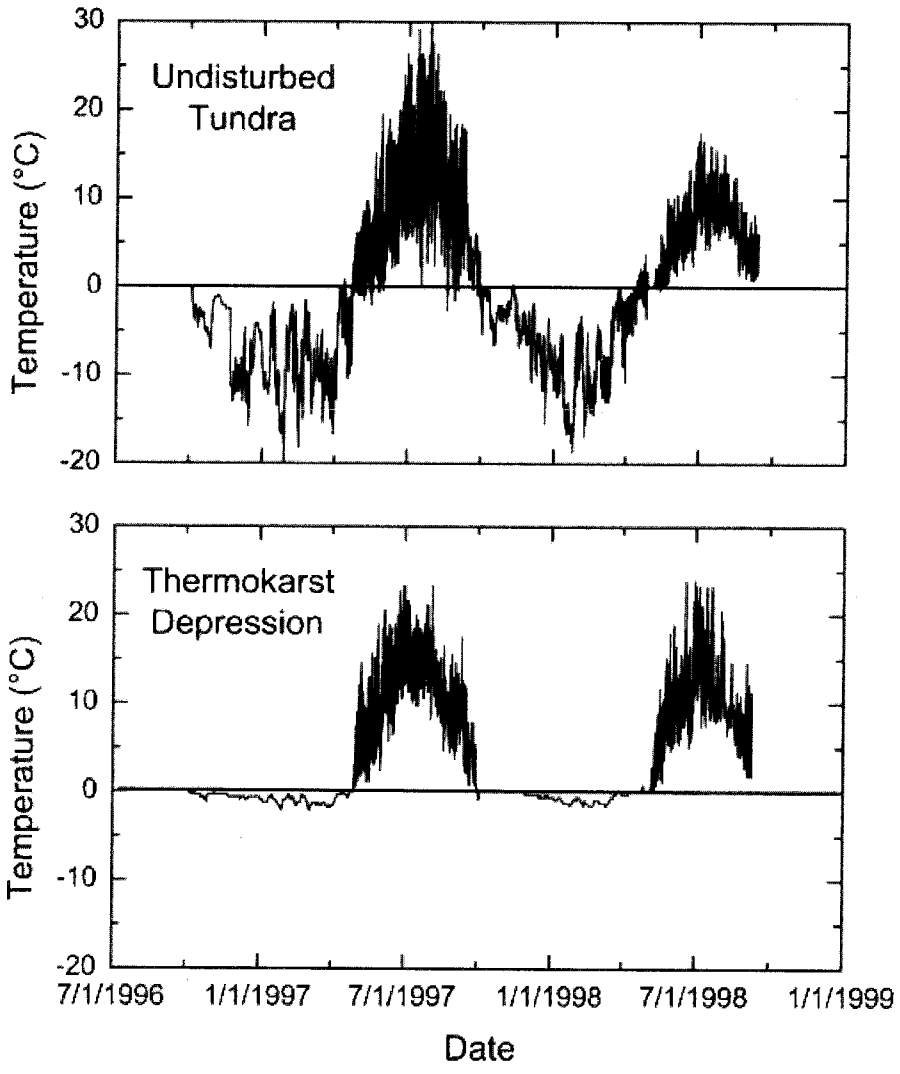

Figure 4 Ground surface temperatures measured five times per day in the Extensive Thaw site in an old thermokarst depression and on the adjacent undisturbed tundra.

DOI: 10.1002/ppp

Table 1 Ground surface temperatures during summer (5/1 to 9/30) and winter (10/1 to 4/30) for four paired sites with measurements made on tundra (T) and in thermokarst depressions (D). These data are for the Extensive Thaw site (old thermokarst) for 1996 to 1998 and for the Moderate Thaw site (borehole site, new thermokarst) for 1995 to 2003

Site	Summer mean	Winter mean	Annual mean
Moderate Thaw T		−5.2°C	
Moderate Thaw D	6.7°C	−1.2°C	2.0°C
Extensive Thaw 1T	8°C	−6.4°	−0.5°C
Extensive Thaw 1D	9.6°C	−0.6°C	3.6°C
Extensive Thaw 2T	8.5°C	−6.7°C	−0.4°C
Extensive Thaw 2D	7.8°C	−0.8°C	2.8°C
Extensive Thaw 3T	8.3°C	−4.3°C	1.0°C
Extensive Thaw 3D	8.0°C	−1.0°C	2.8°C

of thermokarst terrain). This indicates that the effects of any climatic change that result in the onset of thermokarst depressions will be enhanced by snow accumulation in them, a positive feedback effect for permafrost degradation. In the summer, differences between tundra and depressions were small with two of the thermokarst depressions colder (0.3°C and 0.7°C) and one warmer (1.6°C) than the nearby tundra.

Permafrost Surface Temperatures

A comparison of permafrost surface temperatures between undisturbed stable permafrost and degrading permafrost shows a distinct difference in the patterns of winter temperatures. On undisturbed tundra adjacent to the borehole, the permafrost was warm during 1995–98 (annual mean surface temperature −0.5°C) with minimum winter temperatures typically −2 to −3°C and cooler during 1999–2000 with minimum winter temperatures less than −3°C (Figure 5). The permafrost was colder during 2000–01 (−1.1°C) and 2002–03 (−0.9°C). Active-layer freeze-up required 3 to 4 months (mean 104 days) with completion of freeze-up occurring from 10 January to 4 February.

Figure 6 shows temperatures in the depression at 1-m depth about 1 m northwest of the borehole that indicate there was a thin talik between the active layer and the top of the permafrost. Temperatures in the talik were 0°C in winter with summer temperatures <1°C. During winter, the talik was bounded by two-phase

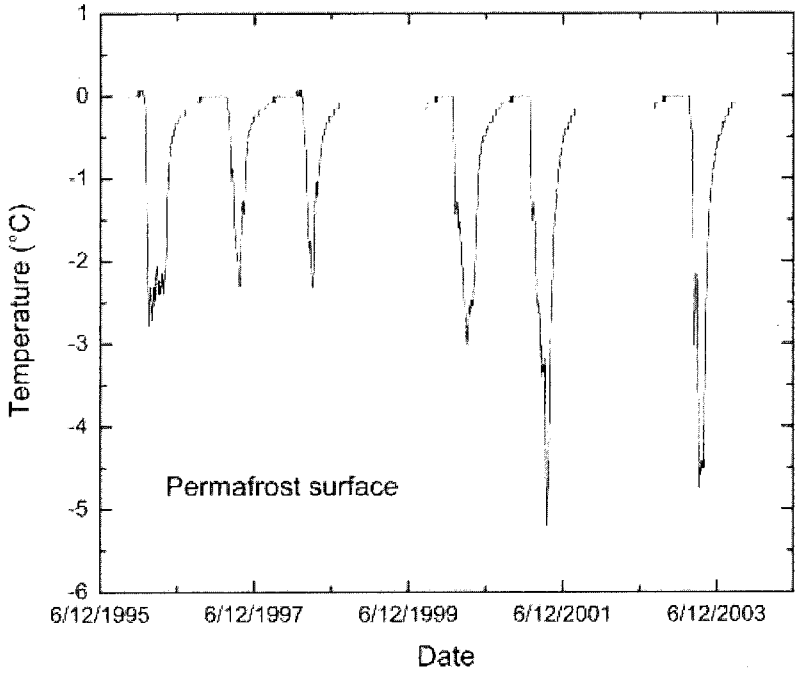

Figure 5 Permafrost surface temperatures measured five times per day in undisturbed tundra near the borehole at the Healy site.

DOI: 10.1002/ppp

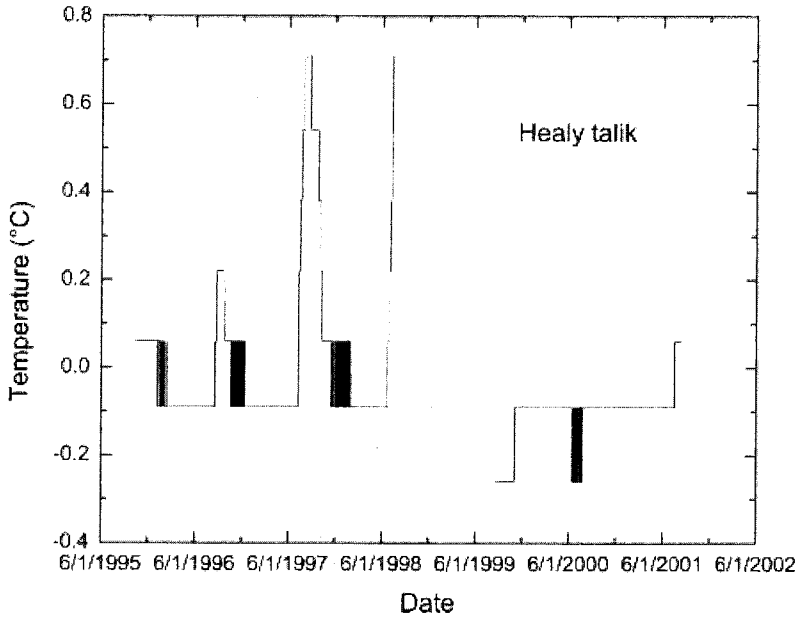

Figure 6 Time series of temperatures measured five times per day at the Healy site adjacent to the borehole at 1-m depth in the talik between the active layer and the permafrost surface. The solid dark areas and step-like changes are a result of resolution of the logger, about 0.15°C.

boundaries (bottom of the seasonal freezing layer and top of the permafrost) that constrained temperatures in this region to 0°C. This decoupled the underlying permafrost from the cold atmosphere so that it could not cool by conductive heat transfer to the surface. Some upward freezing during winter from the permafrost surface into the talik is expected analogous to upward freezing into an active layer during refreezing (Osterkamp and Romanovsky, 1997). Upward freezing would decrease with the decreasing thermal gradient in the underlying permafrost as it warms toward 0°C. During summer, after the seasonally frozen layer thawed, temperatures in the talik increased (Figure 6) allowing for downward heat flow for thawing and warming the underlying permafrost. In the presence of a thin talik, the annual mean permafrost surface temperature remains at or near 0°C and, except for seasonal upward freezing at the permafrost surface, the permafrost can only warm and thaw. Once a talik becomes thicker, the heat flow from it during winter to the active layer above and the permafrost below is insufficient to allow it to cool back to 0°C (T. E. Osterkamp, unpublished work), at which point the permafrost can only warm and thaw.

Deep Permafrost Temperatures

Selected borehole temperature profiles measured during summer (Figure 7) show that the annual mean surface temperature of the permafrost was about −1.4°C in 1989, although it is difficult to determine in such a shallow hole. Annual mean surface temperatures determined from the temperature profiles are spatial averages around the borehole and cannot be compared to point measurements at the surface (Figure 5). There was a net cooling of the permafrost between 1985 and 1989 followed by a strong warming trend at the permafrost surface that began about 1989 or earlier (Figures 7 and 8). The timing of this warming and the rate of temperature increase are similar to those observed at other sites in Interior Alaska (Osterkamp, 2007a). Various extrapolation and curve-fitting methods (Osterkamp, 2005) were used to determine the magnitude of the surface warming (about 1°C) from the measured temperature profiles. The permafrost warmed for a decade (until 1998) and then cooled in general agreement with the point measurements of permafrost surface temperatures. During this decade, new thermokarst terrain was observed forming throughout the area. This warming and thawing of the permafrost with the formation of new thermokarst terrain was coincidental with decreasing air temperatures for the decade (Figure 2), indicating that snow cover or other effects were responsible.

There were increased snow depths during the 1990s (Figure 2) with 6 of 10 years greater than the 1981 to 2001 mean, a condition common throughout Alaska during the late 1980s and early 1990s. Since air temperatures and snow cover effects are the primary

DOI: 10.1002/ppp

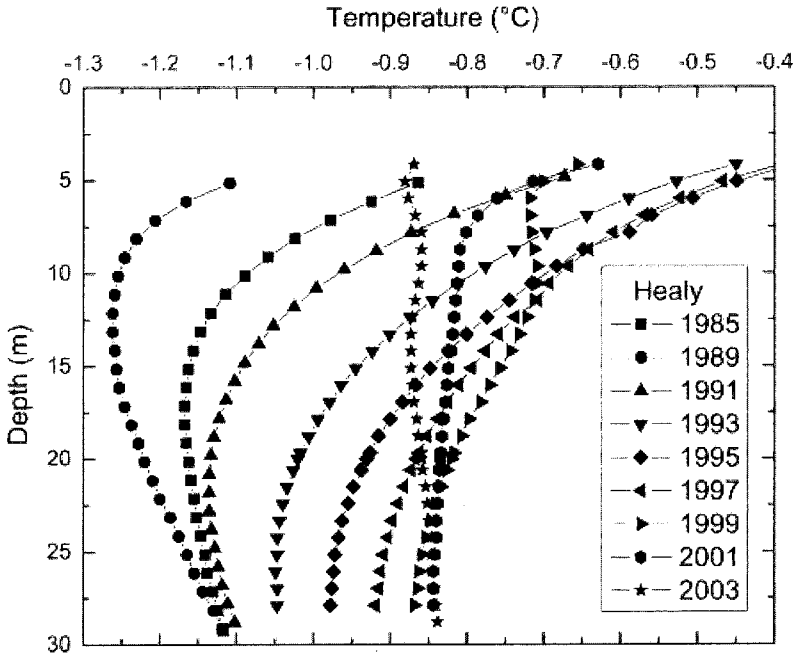

Figure 7 Selected measured temperature profiles (for clarity) at the Healy site for 1985, 1989 and later odd years.

factors controlling ground temperatures, given the decreasing trend in air temperatures, snow cover effects must have played a primary role in warming the permafrost (Osterkamp, 2007b). However, additional factors may have contributed in the immediate vicinity of the borehole including thawing and settling of the ground surface and the eventual formation of a talik there. The formation of new

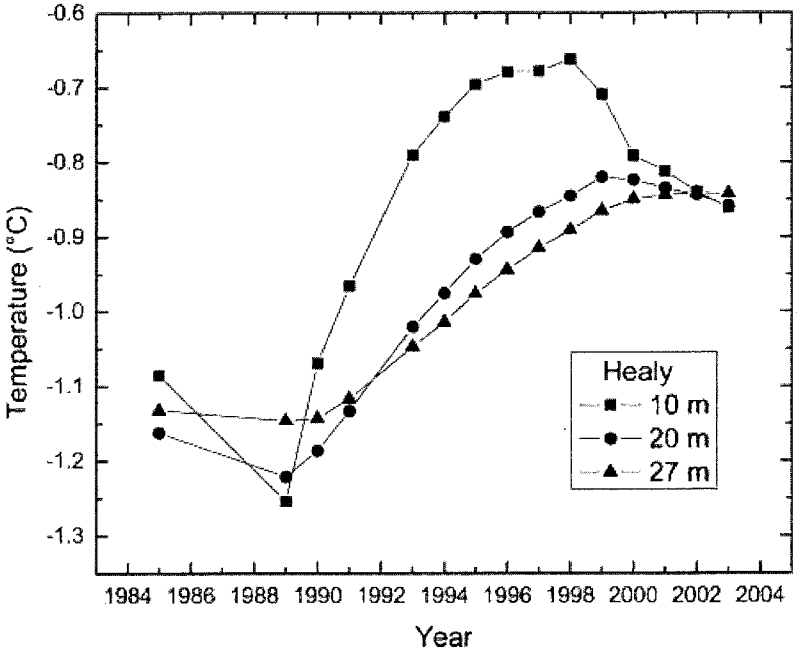

Figure 8 Time series of measured permafrost temperatures at the 10, 20 and 27-m depths at the Healy site.

DOI: 10.1002/ppp

thermokarst terrain away from the borehole must have been a result of snow cover effects. At other permafrost observatories in Alaska, borehole and meteorological data suggest that both snow cover effects and increases in air temperatures were responsible for permafrost warming during the last quarter of the 20th century (Stiegliz *et al.*, 2003; Osterkamp, 2007a, 2008).

Soil Characteristics

Soil properties of undisturbed tussock tundra and the drying tundra adjacent to thermokarst pits were similar (Figure 9). Soil moisture was lowest near the well-drained surface, highest near the bottom of the active layer and remained high within the remaining ~1.5 m due to high ice contents in the permafrost. Bulk density was lowest in the fluffy moss peat, highest in the bottom of the active layer, and gradually increased with depth with decreased organic matter and ice contents. Very low pH and electrical conductivity values near the surface reveal the effects of leaching of cations and the presence of *Sphagnum* mosses. Carbon concentrations were highest in the moss peat near the surface, lower in the thin aeolian silt cap within the active layer and low below 1-m depth where organic matter accumulations were negligible.

Soil profiles from two trenches excavated to a depth of ~1 m reveal a complex soil stratigraphy and soil horizon dislocation (Figure 10). Depth of seasonal thaw at the wall of the pit varied from 0.36 m to 0.43 m. At the wall of pit, the following layers were distinguished: layer 1 was a contemporary sod layer (moss and rootlets); layer 2 was dark-brown peat moderately to well decomposed with a lens of slightly decomposed yellow peat (sub-layer 2a); layer 3 was brown peat moderately decomposed, slightly mineralised with silt and with more dark interlayers which formed a wavy foliation (horizontal or inclined). Sub-layer 3a extended for ~2 m horizontally. At the bottom of this sub-layer, horizontal lenses of brown-grey peaty silt (sub-layer 3b) with varied peat content were exposed. These lenses contained abundant inclusions of gravel (up to 5 cm). At the left part of the section, the silt lens was torn in three sections with the spaces between them filled with peat. At the right part of the section, the silt lens had a mushroom-like shape. Layer 4 was brown peat moderately decomposed, mineralised with silt and with inclusions of gravel. At several sections of the layer, the peat transformed to peaty silt (sub-layer 4a). Layer 5 was grey loam, slightly peaty, with abundant inclusions of gravel. The quantity of inclusions increased with depth and the size of gravel was up to 10 cm.

The structure of the upper part (1 m) of the soil section is a result of slope and cryogenic processes such as solifluction, creep, frost cracking, cryoturbation and others. These processes result in disruption of the sod layer and mixing of organic and mineral horizons within the active layer. The extensive cryoturbation extended from the middle of the active layer into the permafrost beyond the bottom of

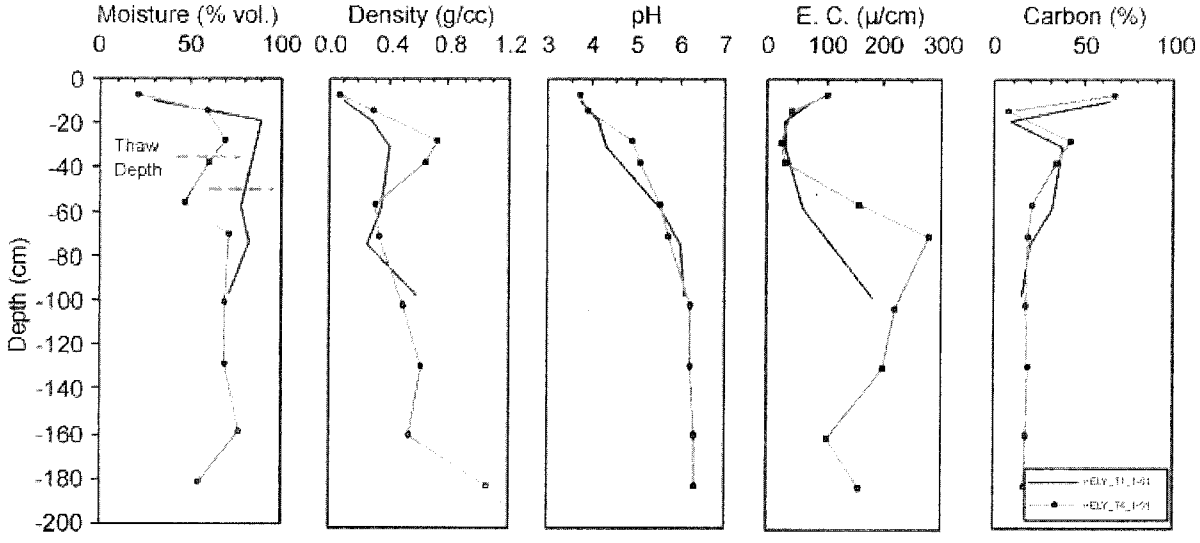

Figure 9 Vertical profiles of moisture, dry density, pH, electrical conductivity (E.C.) and carbon from two shallow soil cores (Figures 1 and 13) at the Healy site.

DOI: 10.1002/ppp

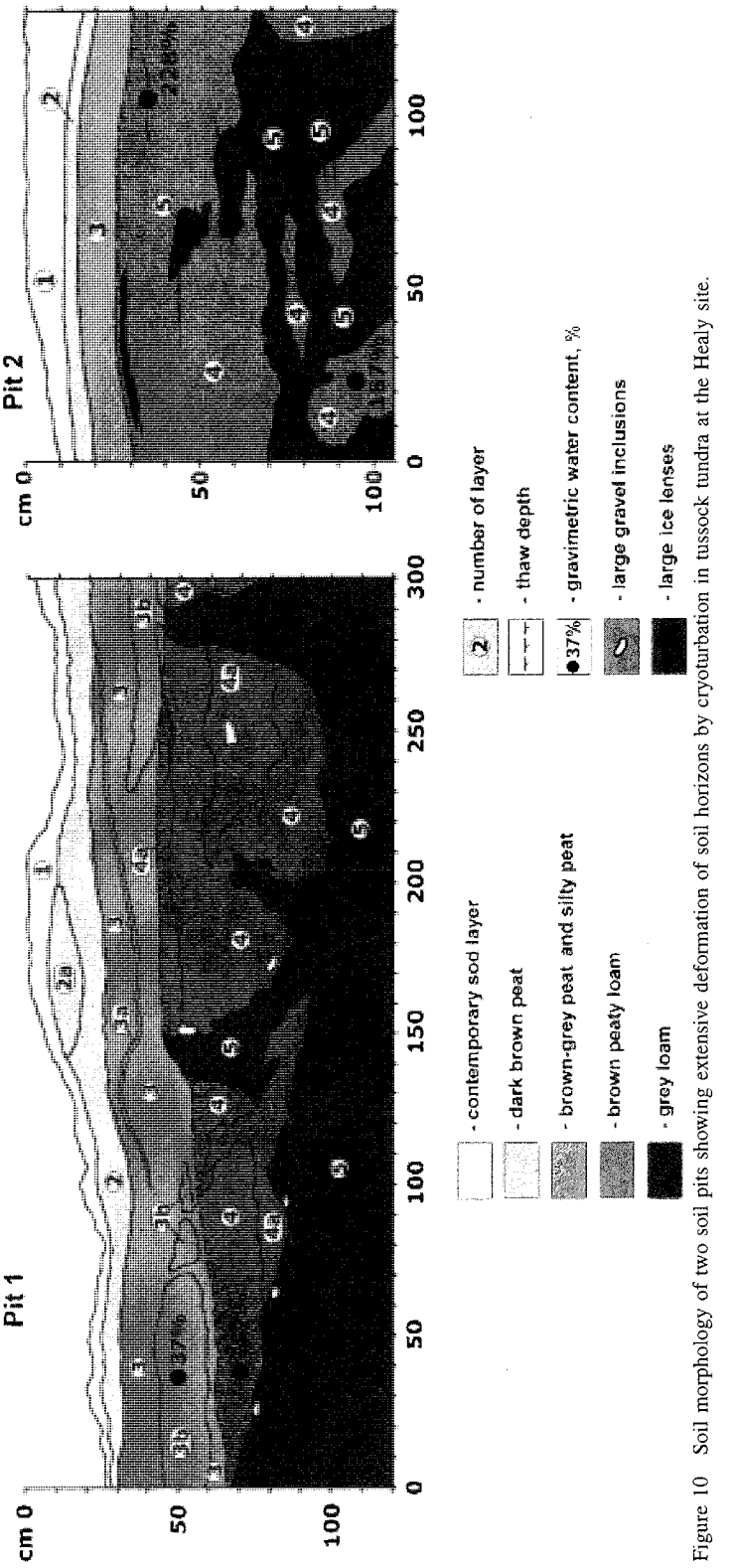

Figure 10 Soil morphology of two soil pits showing extensive deformation of soil horizons by cryoturbation in tussock tundra at the Healy site.

DOI: 10.1002/ppp

the pits, indicating that the active layer once extended to greater depths. In contrast, the surface organic layers showed little disruption, although the boundaries were wavy. Gravel fragments were found throughout the cryoturbated layers but not in the continuous surface organic horizons.

Ground-Ice Characteristics

Ground ice is important in determining whether permafrost develops thermokarst and how thaw settlement affects surface topography and ecosystem responses. Total ice content, distribution with depth and morphology of ground ice all affect surface readjustment. Volumetric water contents in core samples were relatively low in the unsaturated surface organic horizons and uniformly high (mostly 70–80%) in the upper permafrost (Figure 9). Ice contents in the permafrost remain high even with increasing density and mineral content of soils with depth.

Cryostructures in the upper permafrost were classified into five types (Figure 11) and reveal differing formative environments. Pore ice occurs in ice-poor frozen soil at the base of the active layer. This soil was occasionally subject to thawing during years of unusually deep summer thaw. Organic-matrix ice was found in the organic-rich silt (muck). In strongly mineralised sections, cryostructures included lenticular, layered and reticulate. The thickness of the ice layers was typically 0.1 to 0.2 cm and up to 0.7 cm with spacing between ice layers varying from 0.1 to 0.3 cm. The cryostructure of the loam was sub-horizontal wavy lenticular to layered. Ice-layer thicknesses were typically 0.1 to 0.4 cm and up to 1.0 cm. Spacing between ice layers varied from 0.1 to 0.5 cm with a maximum of 1.0 cm. The visible ice content reached 50 per cent.

The distribution and amounts of ground ice (ice contents) were typical of an intermediate layer, an ice-rich quasi-syngenetic horizon in the upper stratum of permafrost (Shur, 1977). Observed features characteristic of this layer included high ice content, prevalence of horizontal (or slightly inclined) ice lenses indifferently crossing lithological boundaries, distinct relatively thick ice layers ('belts') and ataxitic (suspended), lenticular-layered and micro-lenticular cryostructures. This layer was about 1 m thick and was underlain by a thin moderately ice-rich colluvial deposit over glacial till. It appears that formation of the intermediate layer was caused by peat accumulation at the ground surface and consequential reduction of the active-layer thickness by upward freezing from the permafrost surface.

Thawing of the Permafrost

Figure 12 shows the thermokarst pit that developed around the borehole. At the time of the first temperature measurements in 1985, there was no obvious disturbance to the tundra except for the presence of a few shovels of drill cuttings which were removed. At the next site visit 4 years later (1989), the ground around the pipe had settled 0.16 m and there was evidence of thawing (small pits) away from the borehole where there was no activity. As the site evolved, it became clear that the borehole was located at the junction of two water tracks at the upstream end of a thermokarst gully that was forming as a result of natural causes. Aerial photos (see below, Figure 15) and ground observations show that these gullies grow by enlarging and extending upstream along water tracks. Site activities were limited to a few hours annually, largely for gathering temperature data and surveying. While it

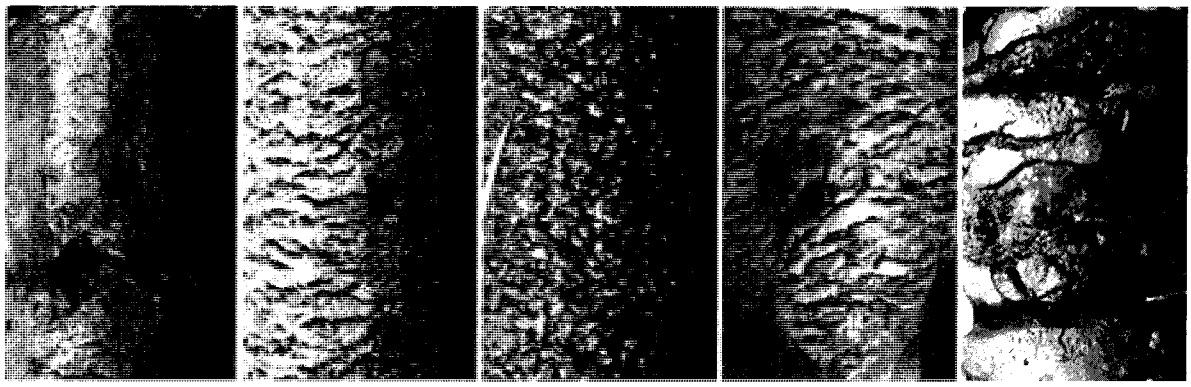

Figure 11 Photographs of ground-ice structures (from left to right) including pore, lenticular, organic matrix, ataxitic (platy inclusions, or braided) and layered ice. Each core is about 8.8 cm in diameter.

DOI: 10.1002/ppp

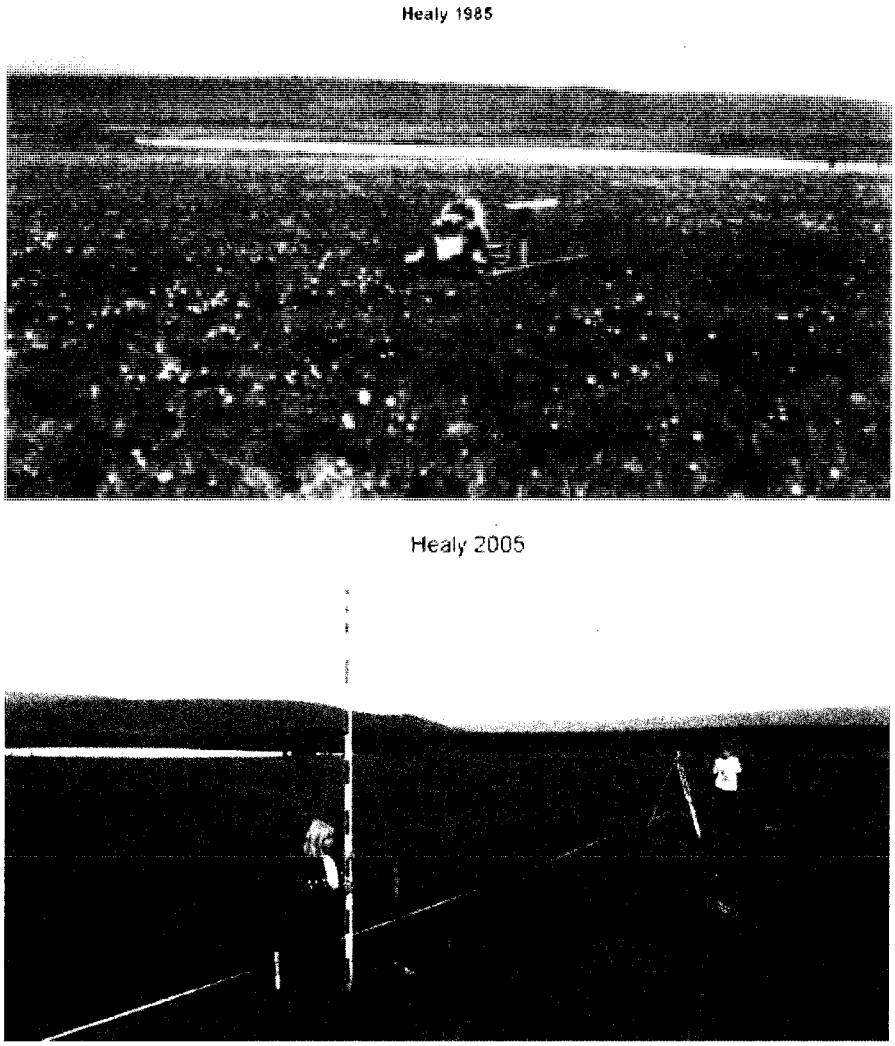

Figure 12 The borehole access pipe at the Healy site in 1985 and 2005 showing the thermokarst pit and changes in vegetation that have developed at the site. The pit is in a thermokarst gully at the junction of two water tracks (Figure 1). These water tracks develop into thermokarst gullies and are a primary mode of permafrost degradation that enlarge and extend upslope with time (Jorgenson and Osterkamp, 2005). This figure is available in colour online at www.interscience.wiley.com/journal/ppp

cannot be determined with certainty if site activities or surface disturbance during drilling played a role in the observed thaw settlement at the borehole, it seems likely that the location of the borehole was primarily responsible for the settlement. Using the pipe as a datum, measurements show that total settlement next to the pipe was about 0.9 m (Figure 13) two decades after the hole was drilled. At its deepest part, total settlement in the pit was about 1.1 m.

Thaw settlement was also evident across the broader landscape as shown by surveys along Transect 1 and across the access pipe over a 7-year period (Figure 13). Up to 0.4 m of thaw settlement occurred between 1996 and 2003, with an average of about 0.24 m. The amount of additional thaw to produce this settlement was estimated from ground-ice measurements obtained from shallow permafrost coring in 2005 (Figure 14) to be about 0.47 m or about 0.07 m permafrost thawed each year.

Rough estimates of the net energy fluxes into the surface of the permafrost at the borehole and along the transect were made based on the amount of thaw settlement and ground-ice contents. The mean thawing rate at the access pipe was approximately

DOI: 10.1002/ppp

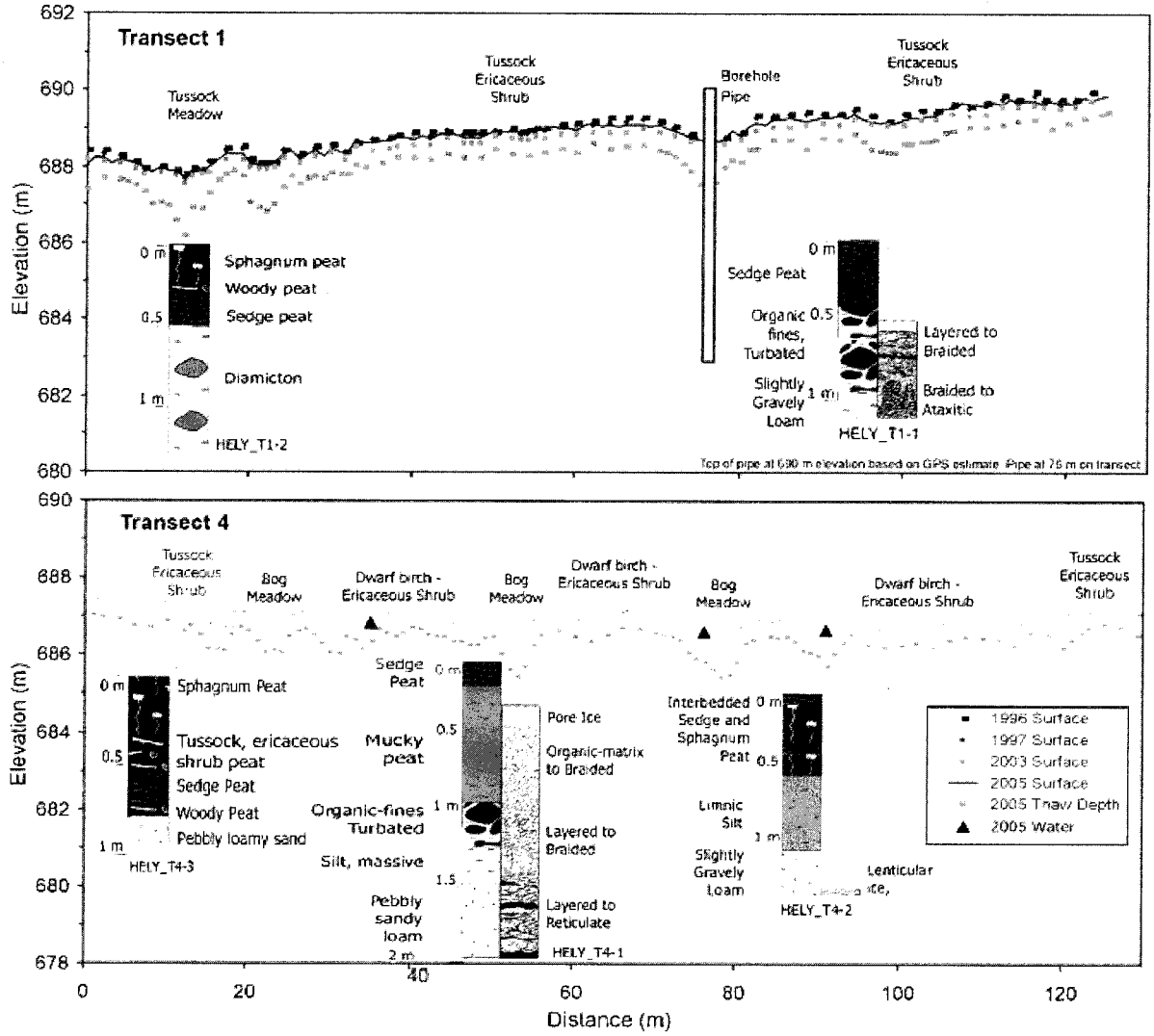

Figure 13 Toposequences of ecological characteristics along transects at the Healy site illustrating ground and water surface elevations, thaw depths, soil stratigraphy and ground-ice profiles, and vegetation. Measurements of the tundra surface in 2005 were made before maximum thaw and later thawing could contribute about 7 cm of additional settlement.

0.1 m/year. With ice contents of 60 per cent, the mean net annual energy flux into the top of the permafrost required to thaw this ice was 0.6 W/m^2. Similarly, the calculated average net annual heat flux into the surface of the permafrost along the transect would have been at least 0.4 W/m^2. This value does not include the energy required to warm the permafrost to the thawing point, warm the soil after thawing and warm the underlying permafrost. It is most likely a result of snow cover effects including drifting into the pit and not a result of climatic warming. The effects of changing vegetation on the energy balance are unknown. For comparison, Osterkamp *et al.* (1994) calculated that a mean energy flux at the permafrost surface of 0.6 to 0.7 W/m^2 was required to produce observed permafrost temperature changes near Prudhoe Bay.

Distribution and Characteristics of Thermokarst Features

Photo-interpretation of the change in characteristics and distribution of thermokarst features on a time series of airphotos from 1954, 1981 and 2005 showed substantial changes in some of the five thermokarst modes observed (Figure 15). Eight Mile Lake (8% of

DOI: 10.1002/ppp

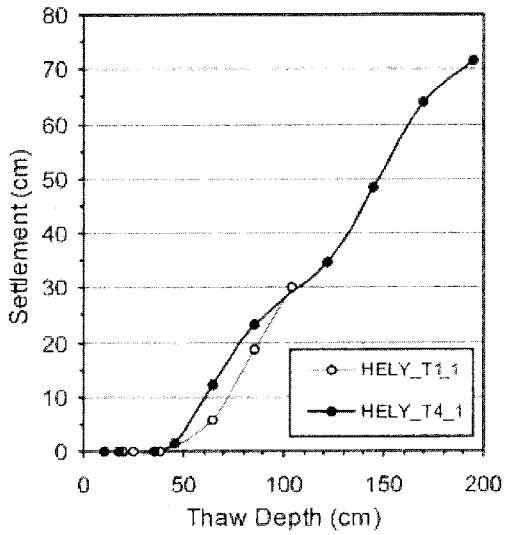

Figure 14 Estimated potential thaw settlement along two transects.

the study area) and its associated shore bogs changed little over time. These bogs are produced by rapid accumulation of *Sphagnum* and sedge peat along the collapsing margins of ice-rich terrain. In contrast, there was a dramatic increase in gullies, from 2.1 per cent to 4.9 per cent of the study area over the 51-year period. The gullies showed a tendency to bifurcate while extending and enlarging upslope (Figure 15). Thermokarst pits and human-induced thermokarst along trails had small but consistent increases. The amount of gully expansion is somewhat uncertain because of the poor quality of the 1954 photography and the lower spatial resolution of the 1954 and 1981 aerial photos but several factors indicate that the increase is real. First, individual trees (as small as 2 m across) are resolvable on both the 1954 and 1981 photos. This indicates that the gullies, which typically were 5–8 m across, should be resolvable if they were present. Second, new gully formation was observed after the beginning of borehole temperature monitoring in 1985. Possibly, the improvement in spectral and spatial quality of the photography exaggerated the measured increase but the expansion of gullies was a real phenomenon.

Response of Vegetation and Soil to Thermokarst

Soil and vegetation sampling and observations made along the upland transect (T1) and the lowland swale transect (T4) indicated dramatic changes in ecological characteristics of tussock tundra in response to thermokarst (Figure 13). These changes included: (1) enhancement of tussock growth in shallow, newly developed thermokarst gullies; (2) replacement of tussock tundra by bog meadows in thermokarst pits; and (3) drying of tussock tundra adjacent to thermokarst pits and gullies and replacement by deciduous and evergreen shrubs. In undisturbed areas,

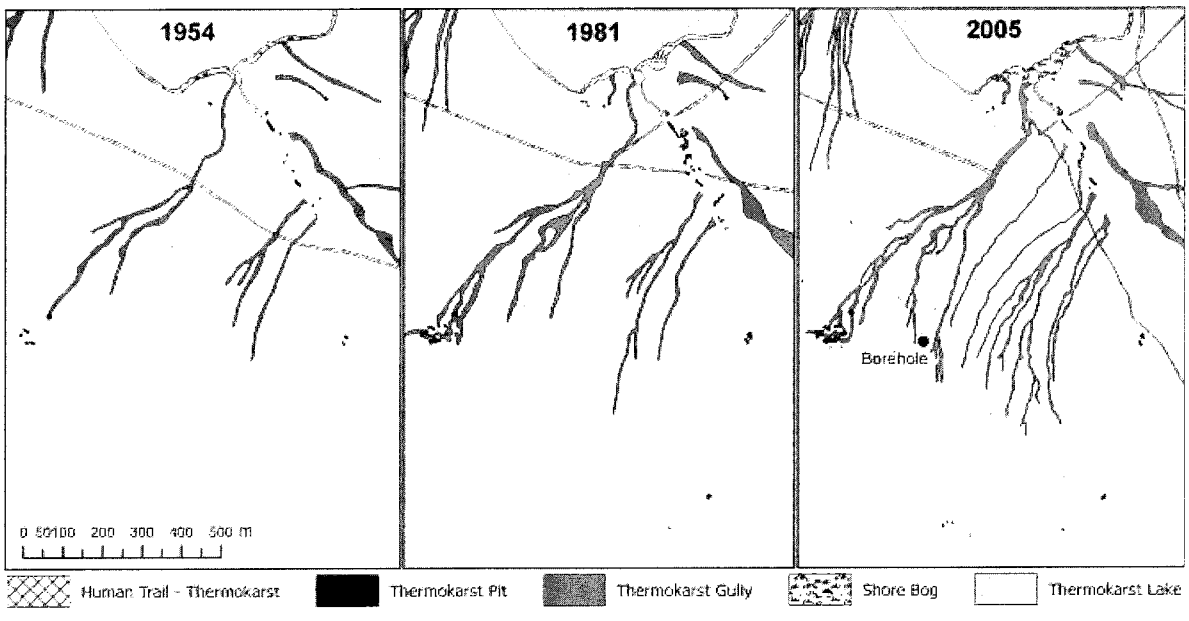

Figure 15 Changes in the distribution of thermokarst features at the Healy site based on photo-interpretation of aerial photography from 1954, 1981 and 2005.

DOI: 10.1002/ppp

tussock tundra was the predominant vegetation across the gentle upland ridges and lower toe slopes of the swales. The soil (Terric Fibristels) of undisturbed tussock tundra (plot T1_1, Figure 13) was moderately well drained, had water at the bottom (−0.47 m) of the shallow (0.49 m) active layer, was extremely acidic (pH = 3.7), had a thick (0.39 m) surface organic horizon and was underlain by a gravelly silt loam developed from glacial till. Vegetation was dominated by *E. vaginatum, B. nana, V. vitis-idaea, V. uliginosum, Empetrum nigrum, S. lenense, Aulacomnium palustre, Dicranum* spp. and *Flavocetraria cucullata.*

In the new thermokarst gully (plot T1_1, Figure 13), vegetation was still dominated by tussock tundra but the tussocks were more robust and darker green, indicative of higher nutrient availability. The soil (Histic Gelaquepts) was poorly drained, had water near the surface (−0.10 m) of a deep thawed layer (up to 1.30 m) and a thick (0.51 m) surface organic horizon. The deep thaw depth indicates that a talik was present because it was too great for typical seasonal thaw. Vegetation was similar to that of undisturbed tussock tundra. *V. uliginosum, S. magelanicum and S. angustifolium* were the dominant mosses instead of *S. lenense.*

In thermokarst pits (plot T4_2, Figure 13) in the swale, bog meadows rapidly colonised the collapsing surface. The soil (Histic Gelaquept) was very poorly drained, had water at the surface (1 cm above), deep thaw depths (>1.37 m) and a thick (0.57 m) surface organic horizon. The deep thaw depths indicate that a talik was present. The peat stratigraphy was complex and included layers of *S. angustifolium*, sedges, *S. fuscum* and ericaceous shrubs that revealed vegetation changes as the pits collapsed. Vegetation showed a large shift in species composition relative to tussock tundra and was dominated by *E. scheuzcheri, Carex rotundata, Sphagnum* (mostly *S. angustifolium*) and *Limpritchia revolvens.* Surface water was abundant.

Tundra areas adjacent to thermokarst pits appeared to be drying and shifting vegetation composition due to lowering of the water table by the settling ground surface in the pits. Such drying also was evident adjacent to deeper incised gullies, such as the Extensive Thaw site. The soil (Typic Aquiturbel) was drained, lacked water within the shallow (0.35 m) active layer, was extremely acidic (pH = 3.7) and had a thin surface (0.18 m) organic horizon. The abundance of ericaceous shrubs and dead and poorly growing tussocks indicate that vegetation has shifted from tussock tundra to deciduous-ericaceous low shrub, presumably due to lowering of the water table. Vegetation was dominated by *V. vitis-idaea, L. decumbens, B. nana, R. chameamorus, E. vaginatum, Dicranum* spp., *Cladina rangiferina* and *C. arbuscula.*

Timing of Vegetation Changes

The timing of permafrost thaw and ecological changes can be investigated through changes in species abundance associated with differing degrees of thermokarst at the Minimal, Moderate and Extensive Thaw sites. Across these sites, abundance of live tussock-forming sedge species *E. vaginatum* decreased, and moss abundance increased with increased permafrost thaw and development of thermokarst terrain (Table 2; Schuur *et al.*, 2007). Hydrophilic *Sphagnum* spp. became increasingly important where thermokarst terrain was present, presumably because the water table in subsided patches was nearer the soil surface. Dead moss (mostly *S. fuscum*) was widespread, especially on higher patches, most likely due to soil moisture

Table 2 Per cent ground cover of various plant groups or species within chambers at the Extensive, Moderate and Minimal Thaw sites

Group	Species	Extensive Thaw site	Moderate Thaw site	Minimal Thaw site
Vascular plants	Tussocks	9.9	38.1	44.7
Non-vascular plants	Hydrophilic *sphagnum*	17.3	8.4	4.7
	Sphagnum fuscum	5.0	9.1	13.5
	Sphagnum magellanicum	18.8	5.1	0.0
	Dicranum spp.	17.6	10.8	8.4
	Feathermoss	1.3	9.4	0.8
	Lichen	8.6	8.8	17.3
	Other moss spp.	2.7	3.0	0.4
	Total	71.3	54.6	45.1
Dead	Tussocks	0.7	0.0	1.7
	Sphagnum spp.	18.1	7.1	7.9

DOI: 10.1002/ppp

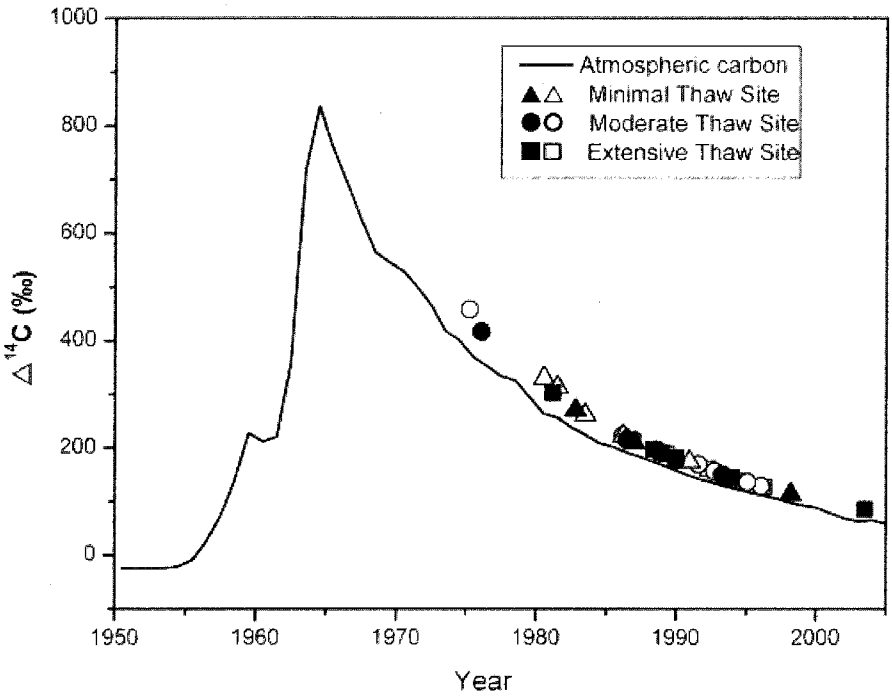

Figure 16 Radiocarbon content of the northern hemisphere atmosphere and radiocarbon measurements from dead moss sampled at the Healy permafrost thawing sites in 2003 (open symbols) and 2005 (closed symbols) vs the inferred last year of growth. The estimated final year of growth of these moss patches ranged from 1975 to 2004, with a concentration of dates between 1985 and 1995.

redistribution as a result of nearby ground subsidence. The Extensive Thaw site had twice as much dead moss and the proportions of *S. fuscum* dead in each area were: Extensive Thaw, 78 per cent, Moderate Thaw, 44 per cent and Minimal Thaw, 37 per cent (Table 2).

Radiocarbon measurements provided an independent estimate of when these changes in vegetation took place by recording the year that individual moss patches died. There was a large range in radiocarbon content measured in surface dead *Sphagnum* moss across all three sites with all samples elevated relative to the contemporary atmosphere (Figure 16), indicating that the mosses died some years prior to the collection period. The estimated final year of growth of these moss patches ranged from 1975 to 2004, with a concentration of dates between 1985 and 1995 (Figure 16). The average last year of growth for all samples across sites was 1989, and was the same if 2003 and 2005 samples were averaged separately. At the Minimal Thaw site, the average age of the final year's growth was 1985 ± 1.9 years in the 2003 samples and 1989 ± 4.6 years in the 2005 samples. At the Extensive Thaw site, the average did not change between 2003 (1991 ± 1.7 years) and 2005 sampling (1991 ± 3.0 years), while the Moderate Thaw site changed slightly, but not significantly, from 1989 ± 2.7 years in 2003 to 1987 ± 2.9 years in 2005. Considering only the 2005 samples as the more accurate age distribution, both the Extensive and Moderate Thaw sites had a cluster of dates between 1986 and 1994, whereas the Minimal Thaw site, with less dead moss, had only three dates that were relatively evenly spaced through time.

Warming of the permafrost at the borehole (Moderate Thaw site) started in 1989 or earlier in good agreement with the final years of moss growth at all sites. Exact agreement is not expected because the moss measurements were made over a broad area, while the borehole temperatures are indicative of changes in the immediate area around the hole. These data suggest that once ice-rich permafrost began to degrade water was redistributed towards the subsiding thermokarst depressions causing adjacent higher areas to become drier. This resulted in a reduced water supply to the moss which would have caused it to die.

SUMMARY

Observations and measurements at a tundra site near Healy, Alaska since 1985 reveal a cascading sequence of permafrost, ecological, hydrological and other

DOI: 10.1002/ppp

changes. The timing and amount of permafrost degradation were closely associated with changing permafrost temperatures, ground-ice characteristics, active-layer dynamics and accumulation of snow in thermokarst features (pits, ponds and gullies). Permafrost degradation altered surface topography, surface and ground water levels, and channelisation of surface runoff in gullies. Differential thaw settlement and redistribution of water caused shifts in vegetation and peat accumulation in response to wetting and drying.

Permafrost at the site is classified as climate-driven, ecosystem protected (Shur and Jorgenson, 2007) because the permafrost was formed under an earlier cold climate independent of ecological conditions and later protected from degradation by vegetation and soil development. Included in this concept is the modification of permafrost characteristics as ecosystems evolved over time that increases ice contents and makes the permafrost more sensitive to thermokarst.

Borehole temperatures measured at the site cooled slightly from 1985 to 1989. The annual mean permafrost surface temperature was about −1.4°C in 1989. On undisturbed tundra adjacent to the borehole, annual mean permafrost surface temperatures ranged from −0.5°C to −1.1°C (1995–2003), with the lower temperatures occurring in the latter part of the period. There was a warming of about 1°C (1989–98). The period of permafrost warming coincided with a decreasing trend in air temperatures (about 0.1°C per year, 1985 through 1999). Decreasing air temperatures could not have caused the increase in permafrost temperatures or new thermokarst terrain. Snow cover was substantially above average during this period and must have played a significant role in warming and thawing the permafrost and in the formation of new thermokarst terrain (Osterkamp, 2007b). Permafrost warming at this site is consistent with broader observations of permafrost warming during the 20th century and during the last quarter of the century (Lachenbruch and Marshal, 1986; Osterkamp, 2007a).

Ground-ice distribution and contents were typical for an intermediate layer: an ice-rich quasi-syngenetic horizon at the upper stratum of permafrost. This layer appears to have formed as a result of peat accumulation and consequent reduction of the active-layer depth by upward freezing from the permafrost. The accumulation of substantial amounts of excess ice in the intermediate layer makes it sensitive to thaw with alteration of surface topography by differential settlement.

Thermokarst development in response to climatic change and permafrost thawing was evident from field observations and remote sensing. Ground photos, topographic surveying and temperature measurements documented the development of a thermokarst pit at the borehole and along an adjacent transect. A talik developed adjacent to the borehole, as indicated by the constant measured winter temperature of 0°C. The talik decouples the permafrost from the cold atmosphere so that it cannot cool by conductive heat transfer to the atmosphere and can only warm and thaw. Topographic surveys along a toposequence showed thaw settlement due to permafrost thawing over a 7-year period averaged about 0.24 m. This required an average net annual heat flux into the surface of the permafrost of at least 0.4 W/m^2. Interpretation of airphotos (1954, 1981 and 2005) showed a substantial increase in thermokarst gullies, from 2.1 per cent to 4.9 per cent of the study area over the 51-year period. These gullies showed a tendency to bifurcate while enlarging and extending upslope (Figure 15). There was little change in shore bogs along Eight Mile Lake. Thermokarst pits and human-induced thermokarst along trails had small increases. A few small thermokarst ponds were already present in 1954 and these may have formed in the late 1930s to early 1940s in response to warm air temperatures and thick snow covers during that period.

Thermokarst terrain caused substantial changes in annual mean ground surface temperatures. Temperatures in thermokarst depressions were 2–4°C warmer than nearby tundra, primarily due to winter mean temperatures that were 3–6°C warmer and close to 0°C in the depressions. This was caused, in part, by redistribution of snow (by wind) that accumulated in the depressions and insulated the ground surface from low air temperatures. Such a positive snow-thermokarst feedback effect would enhance the effects of any climatic change (that creates thermokarst depressions) on permafrost.

Soil and vegetation associated with tussock tundra have undergone dramatic changes in response to thermokarst. These changes include: (1) enhancement of tussock growth in shallow, newly developed thermokarst gullies; (2) replacement of tussock tundra by bog meadows in thermokarst pits at later stages of thermokarst development; (3) drying of tussock tundra adjacent to thermokarst pits and well-developed gullies and replacement by deciduous and ericaceous shrubs at later stages of thermokarst development; and (4) mortality of mosses during initial stages of thaw settlement, and a shift in moss species abundance and relative productivity between thermokarst terrain and undisturbed areas. Overall, abundance of live tussock-forming sedge species *E. vaginatum* decreased and moss abundance increased with development of thermokarst terrain. Dead moss (mostly *S. fuscum*) was widespread, especially on higher patches, most

DOI: 10.1002/ppp

likely due to soil moisture redistribution as a result of nearby ground subsidence.

Timing of thermokarst occurrence was evaluated through field observations, borehole temperature measurements and radiocarbon dating of dead mosses. The average final year of growth of the dead moss patches was 1989 (range 1975 to 2004), with dates concentrated between 1985 and 1995. Small thermokarst pits were observed in 1989 and warming of permafrost at the borehole started in 1989 or earlier in approximate agreement with the final years of growth at all sites.

Our interpretation of these observations and measurements is that permafrost, active layer and ground-ice conditions at the Healy site are the combined result of the relative roles of climatic and ecologic factors operating over a long time. Accumulation of ground ice leads to long-term differential frost heave creating a related microrelief. When ground ice in the permafrost melts, the ground surface settles resulting in thermokarst terrain (pits and gullies) that substantially modifies the relief. Windblown snow fills the initial thermokarst depressions causing further warming and thawing of the underlying permafrost, a positive feedback effect that enhances permafrost degradation. Changes in the relief alter the near-surface hydrology and ecological processes. Vegetation changes include differential tussock growth and mortality and a shift in moss species abundance and relative productivity, depending on microtopographic position created by the thermokarst terrain. Water redistribution towards thermokarst depressions causes them to become wetter and adjacent higher areas to become drier, increasing moss mortality and shrub abundance.

NOTATION

h_i	thickness of a i'th sub-layer before thawing and settling, m.
H_1	active-layer depths before thawing and settling, m.
H_2	active-layer depths after thawing and settling, m.
ΔH_i	thickness of the sub-layer h_i after thawing and settling, m.
S	potential thaw settlement, m.
ΔS_i	thaw settlement of the i'th layer, m.
γ_{df}	dry density of the frozen soil sample, kg/m^3.
γ_{dt}	dry density of the thawed and consolidated sample, kg/m^3.
δ	thaw strain.
δ_i	thaw strain of the i'th layer.

ACKNOWLEDGEMENTS

This research was supported by the following grants: NSF (DEB-0516326, DEB-0747195, ARC-0454939, ARC-0454985, ARC-0520578); LTER (0080609); NASA NIP (02-0000-0075) by the Army Research Office, the US Department of Energy (NIGEC) and the State of Alaska. We wish to thank Mr Tom George, Dr Olga Afonina, Hanna Lee, Karen Jorgenson, Eric Jorgenson and Joan Osterkamp for their help with the field research.

REFERENCES

Bowling SA. 1990. Problems with the use of climatological data to detect climatic change at high latitudes. In *Proceedings of the International Conference on the Role of Polar Regions in Global Change*, Vol. 1 Univ. of Alaska: Fairbanks, AK; 206–209.

Brown J, Grave NA. 1979. Physical and thermal disturbance and protection of permafrost. US Army Cold Regions Research and Engineering Laboratory, Hanover, NH. Special Report 79-5, 42 pp.

Clow GD, Urban FE. 2002. Largest permafrost warming in northern Alaska during the 1990s determined from GTN-P borehole temperature measurements. *EOS Trans. AGU* **83**(47): F258.

Crory FE. 1973. Settlement associated with the thawing of permafrost. In *Permafrost: The North American Contribution to the Second International Conference*, Yakutsk, Siberia, USSR. National Academy of Sciences: Washington, DC; 599–607.

Froese DG, Westgate JA, Reyes AV, Enkin RJ, Preece SJ. 2008. Ancient permafrost and a future, warmer Arctic. *Science* **321**: 1648. doi: 10.1126/science.1157525.

Gaudinski JB, Dawson TE, Quideau S, Schuur EAG, Roden JS, Trumbore SE, Sandquist DR, Oh SW, Wasylishen RE. 2005. Comparative analysis of cellulose preparation techniques for use with C-13, C-14, and O-18 isotopic measurements. *Analytical Chemistry* **77**: 7212–7224.

Hansen J, Lebedev S. 1987. Global trends of measured surface air temperatures. *Journal of Geophysical Research* **92**(D11), 13,345–13,372.

Huntington HP. 1992. *Wildlife Management and Subsistence Hunting in Alaska*. Belhaven Press: London; 177 pp.

Huscroft CA, Lipovsky PS, Bond JD. 2004. A regional characterization of landslides in the Alaska Highway corridor, Yukon. Yukon Geological Survey, Whitehorse. Open File 2004-18.

Jorgenson MT, Osterkamp TE. 2005. Response of boreal ecosystems to varying modes of permafrost degradation in Alaska. *Canadian Journal of Forest Research* **35**: 2100–2111.

Jorgenson MT, Racine CH, Walters JC, Osterkamp TE. 2001. Permafrost degradation and ecological changes

associated with a warming climate in central Alaska. *Climatic Change* **48**(4): 551–579.

Jorgenson MT, Shur YL, Pullman ER. 2006. Abrupt increase in permafrost degradation in Arctic Alaska. *Geophysical Research Letters* **33**: L02503. DOI: 10.1029/2005GL024960.

Jorgenson MT, Yoshikawa K, Kaveskiy M, Shur YL, Romanovsky V, Marchenko S, Grosse G, Brown J, Jones B. 2008. Permafrost characteristics of Alaska. In *Proceedings of the 9th International Conference on Permafrost, Fairbanks, Alaska, Extended Abstracts*, Kane D, Hinkel K (eds). Univ. of Alaska: Fairbanks; 121–122.

Kershaw GP. 2008. Snow and temperature relationships on polygonal peat plateaus, Churchill, Manitoba, Canada. In *Proceedings of the 9th International Conference on Permafrost, Fairbanks, Alaska*, Vol. 1 Kane DL, Hinkel KM (eds). Univ. of Alaska: Fairbanks; 925–930.

Lachenbruch AH, Marshall BV. 1986. Changing climate: Geothermal evidence from permafrost in the Alaskan Arctic. *Science* **234**: 689–696.

Lachenbruch AH, Cladouhos TT, Saltus RW. 1988. Permafrost temperatures and the changing climate. In *Proceedings of the 5th International Conference on Permafrost, Trondheim, Norway*, vol. 3, Senneset K (ed.). Tapir Publishers: Trondheim, Norway; 9–17.

Levin I, Kromer B. 1997. Twenty years of atmospheric (CO2)-C-14 observations at Schauinsland station. Germany. *Radiocarbon* **39**: 205–218.

Osterkamp TE. 1994. Evidence for warming and thawing of discontinuous permafrost in Alaska. *EOS Trans. AGU* **75**(44): 85.

Osterkamp TE. 2003a. A thermal history of permafrost in Alaska. In *Proceedings of the 8th International Conference on Permafrost*, Vol. 2, Phillips M, Springman SM, Arenson LU (eds). AA Balkema: Lisse, The Netherlands; 863–868.

Osterkamp TE. 2003b. Establishing long-term permafrost observatories for active layer and permafrost investigations in Alaska: 1977–2002. *Permafrost and Periglacial Processes* **14**(4): 331–342. DOI: 10.1002/ppp.464

Osterkamp TE. 2005. The recent warming of permafrost in Alaska. *Global and Planetary Change* **49**: 187–202.

Osterkamp TE. 2007a. Characteristics of the recent warming of permafrost in Alaska. *Journal of Geophysical Research* **112**: F02S02. doi:10.1029/2006JF000578

Osterkamp TE. 2007b. Causes of warming and thawing permafrost in Alaska. *EOS* **88**: (48), 3–4, 27 November.

Osterkamp TE. 2008. Thermal state of permafrost in Alaska during the fourth quarter of the twentieth century, invited plenary paper. In *Proceedings of the 9th International Conference on Permafrost, Fairbanks, Alaska*, Vol. 2, Kane DL, Hinkel KM (eds). Univ. of Alaska: Fairbanks; 1333–1338.

Osterkamp TE, Jorgenson J. 2006. Warming of permafrost in the Arctic National Wildlife Refuge. *Permafrost and Periglacial Processes* **17**: 65–69. DOI: 10.1002/ppp.538

Osterkamp TE, Jorgenson MT. 2009. Permafrost conditions and processes. In *National Park Service Geological Monitoring Manual*, Young R, Thompson H (eds). Geological Society of America: Boulder, Co.: In press.

Osterkamp TE, Romanovsky VE. 1997. Freezing of the active layer on the Coastal Plain of the Alaskan Arctic. *Permafrost and Periglacial Processes* **8**: 23–44.

Osterkamp TE, Romanovsky VE. 1999. Evidence for warming and thawing of discontinuous permafrost in Alaska. *Permafrost and Periglacial Processes* **10**: 17–37.

Osterkamp TE, Zhang T, Romanovsky VE. 1994. Evidence for a cyclic variation of permafrost temperatures in Northern Alaska. *Permafrost and Periglacial Processes* **5**: 137–144.

Osterkamp TE, Esch DC, Romanovsky VE. 1997. Infrastructure: Effects of climatic warming on planning, construction and maintenance. In *Proceedings of the BESIS Workshop*. Center for Global Change and Arctic System Research, Univ. of Alaska: Fairbanks, AK.

Osterkamp TE, Viereck L, Shur YL, Jorgenson MT, Racine CH, Doyle AP, Boone RD. 2000. Observations of thermokarst in boreal forests in Alaska. *Arctic, Antarctic, and Alpine Research* **32**(3): 303–315.

Schuur EAG, Crummer KG, Vogel JG, Mack MC. 2007. Plant species composition and productivity following permafrost thaw and thermokarst in Alaskan tundra. *Ecosystems* **10**: 280–292.

Shur Y. 1988. The upper horizon of permafrost soil. In *Proceedings of the 5th International Conference on Permafrost*, Vol. 1, Senneset K (ed.). Tapir Pub.: Trondheim, Norway; 867–871.

Shur YL. 1977. *Thermokarst: On the thermo-physical fundamentals of the development of the process* (in Russian). Nedra: Moscow; 98 pp.

Shur YL, Jorgenson MT. 1998. Cryostructure development on the floodplain of the Colville River Delta, Northern Alaska. In *Proceedings of the 7th International Permafrost Conference, Collection Nordicana, no. 57*. Univ. Laval, Sainte-Foy: Quebec; 993–1000.

Shur YL, Jorgenson MT. 2007. Patterns of permafrost formation and degradation in relation to climate and ecosystems. *Permafrost and Periglacial Processes* **18**: 7–19. doi: 10.1002/ppp.582

Shur YL, Osterkamp TE. 2007. Thermokarst. Rept. INE06.11, Inst. of Northern Eng., Univ. of Alaska, Fairbanks, AK, 50 pp.

Stieglitz M, Dery SJ, Romanovsky VE, Osterkamp TE. 2003. The role of snow cover in the warming of arctic permafrost. *Geophysical Research Letters* **30**(13): **1721**: doi:10.1029/2003GL017337.

Stuiver M, Polach HA. 1977. Reporting of C-14 data – discussion. *Radiocarbon* **19**: 355–363.

Vitt DH, Halsey LA, Zoltai SC. 2000. The changing landscape of Canada's western boreal forest: the current dynamics of permafrost. *Canadian Journal of Forest Research* **30**(2): 283–287.

Washburn AL. 1978. *Geocryology: A survey of periglacial processes and environments*. John Wiley and Sons, Inc.: New York, NY; 406 pp.

Zhang T, Osterkamp TE. 1993. Changing climate and permafrost temperatures. In *Proceedings of the 6th International Conference on Permafrost*, 5–9 July. South China University of Technology Press: Wushan, Guangzhou, PRC; 783–788.

Zhang T, Barry RG, Knowles K, Heginbottom JA, Brown J. 1999. Statistics and characteristics of permafrost and ground ice distribution in the Northern Hemisphere. *Polar Geography* **23**(2): 132–154.

DOI: 10.1002/ppp